Supplementary Information

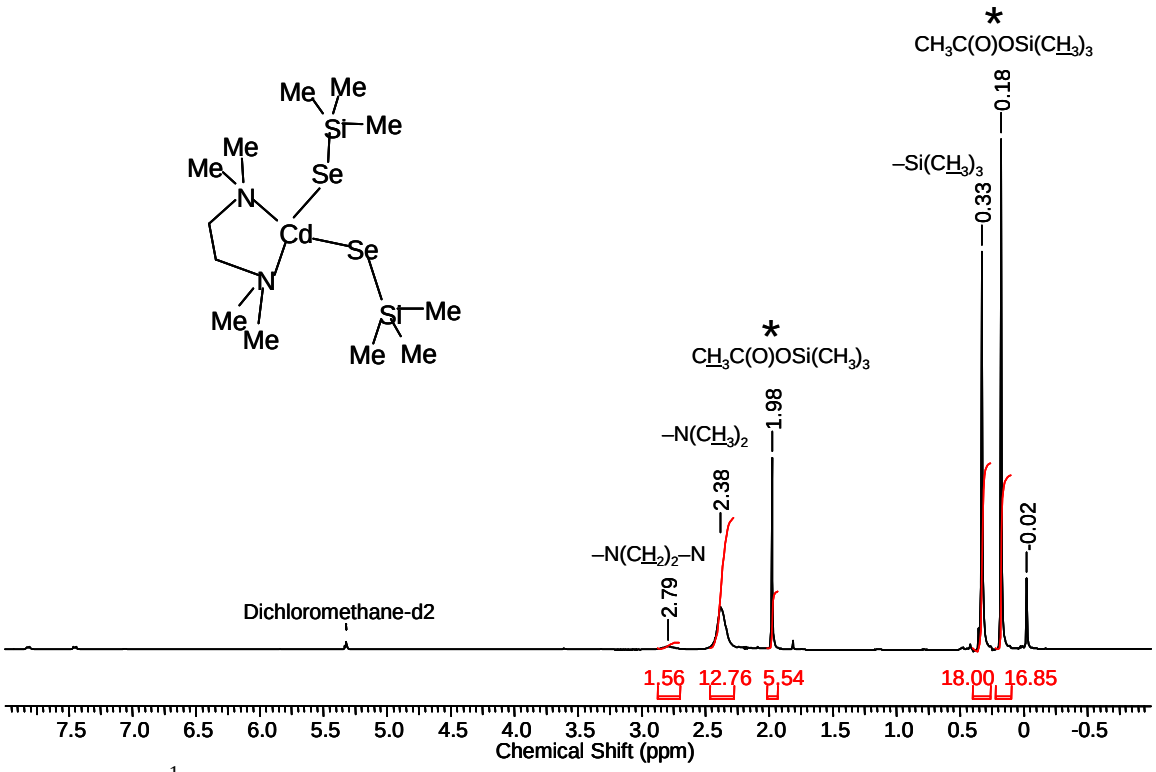

Figure S1. ^{1}H NMR spectrum of the reaction solution for the synthesis of [(*N*,*N'*-tmeda)Cd(SeSiMe$_3$)$_2$ in CD$_2$Cl$_2$. The peaks corresponding to the anticipated side product AcOSiMe$_3$ are identified by (*).

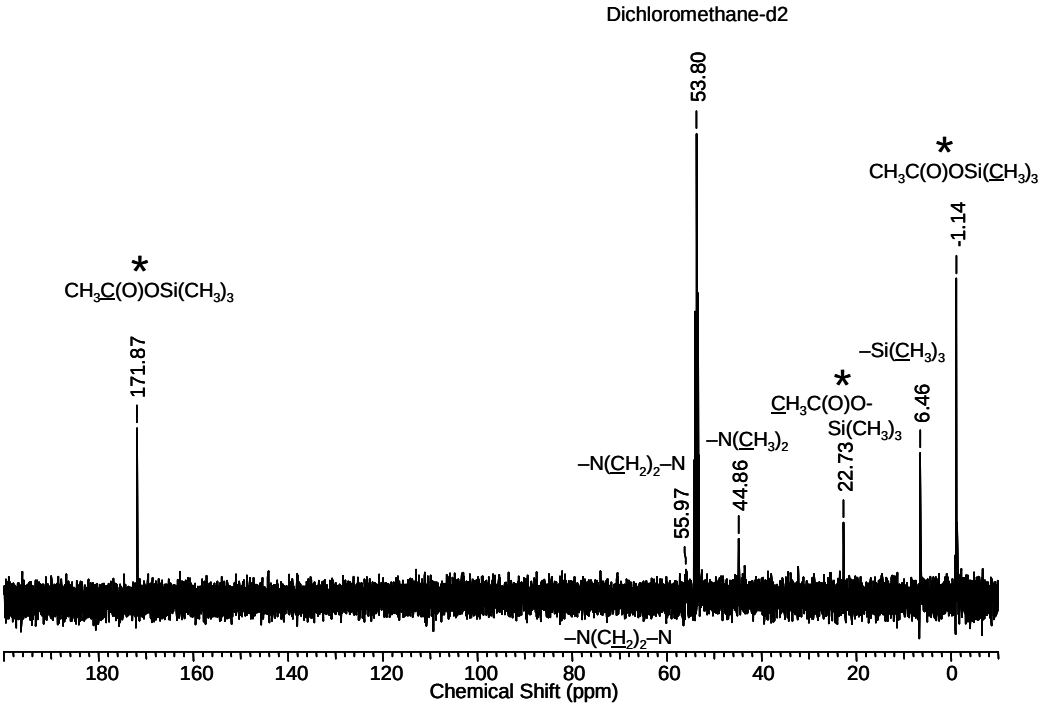

Figure S2. ^{13}C NMR spectrum of the reaction solution for the synthesis of [(*N*,*N'*-tmeda)Cd(SeSiMe$_3$)$_2$ in CD$_2$Cl$_2$. The peaks corresponding to the anticipated side product AcOSiMe$_3$ are identified by (*).

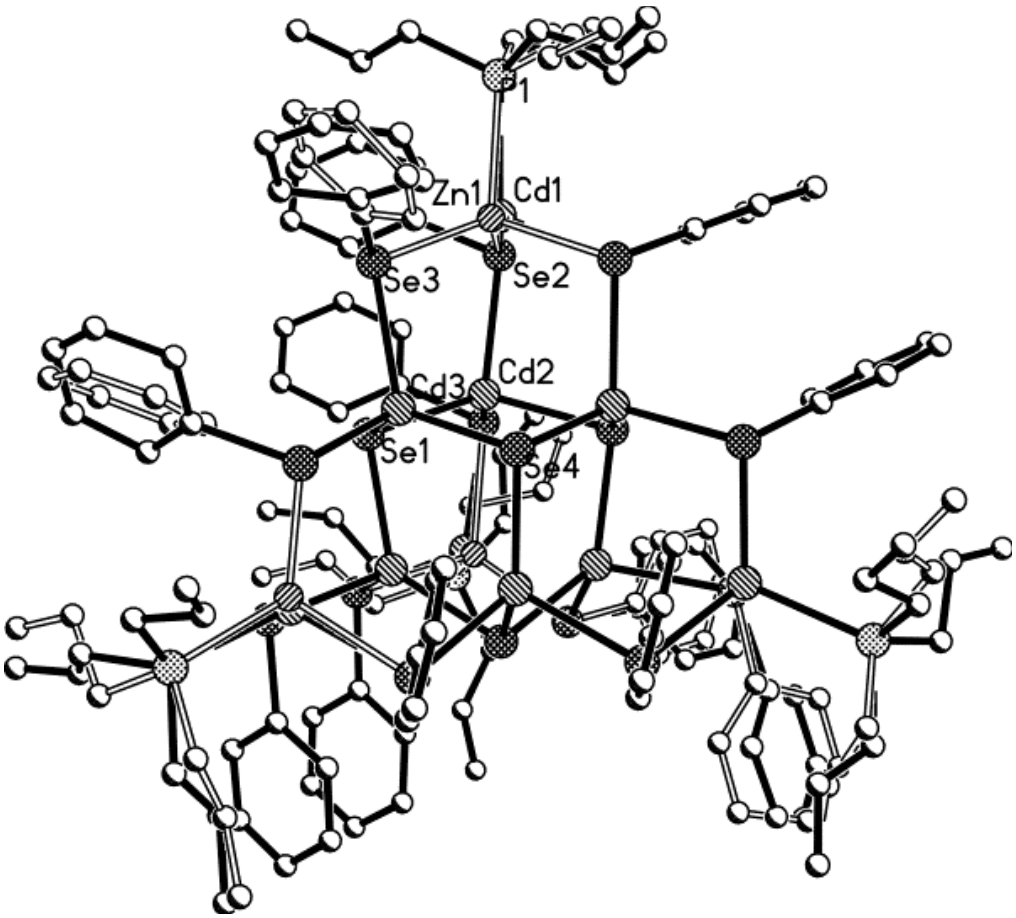

Figure S3. The molecular structure of $[Zn_{1.8}Cd_{8.2}Se_4(SePh)_{12}(P^nPr_3)_4]$ (**2a**) showing the Zn1/Cd1 disorder at the site of highest Zn concentration (30% site occupancy). Disordered carbon atoms of the P^nPr_3 and –SePh ligands are depicted by open bonds.

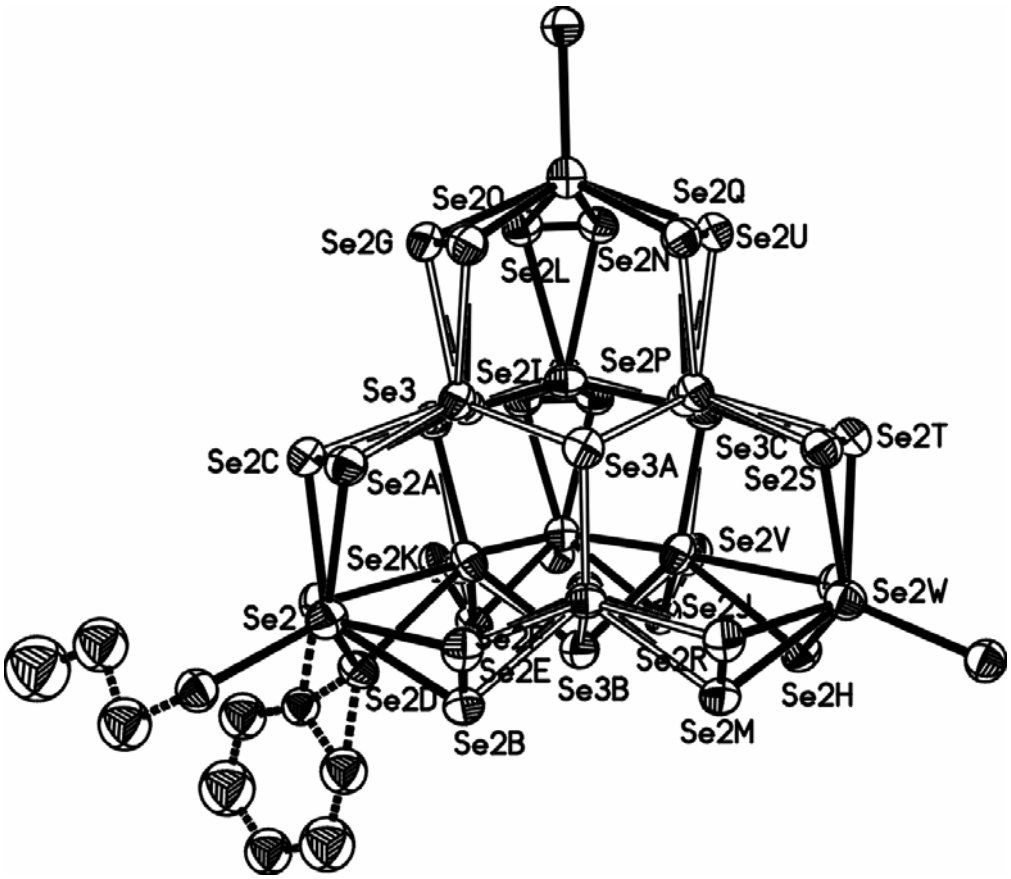

Figure S4. Molecular structure of complex **5** showing the disorder of the selenium atoms.

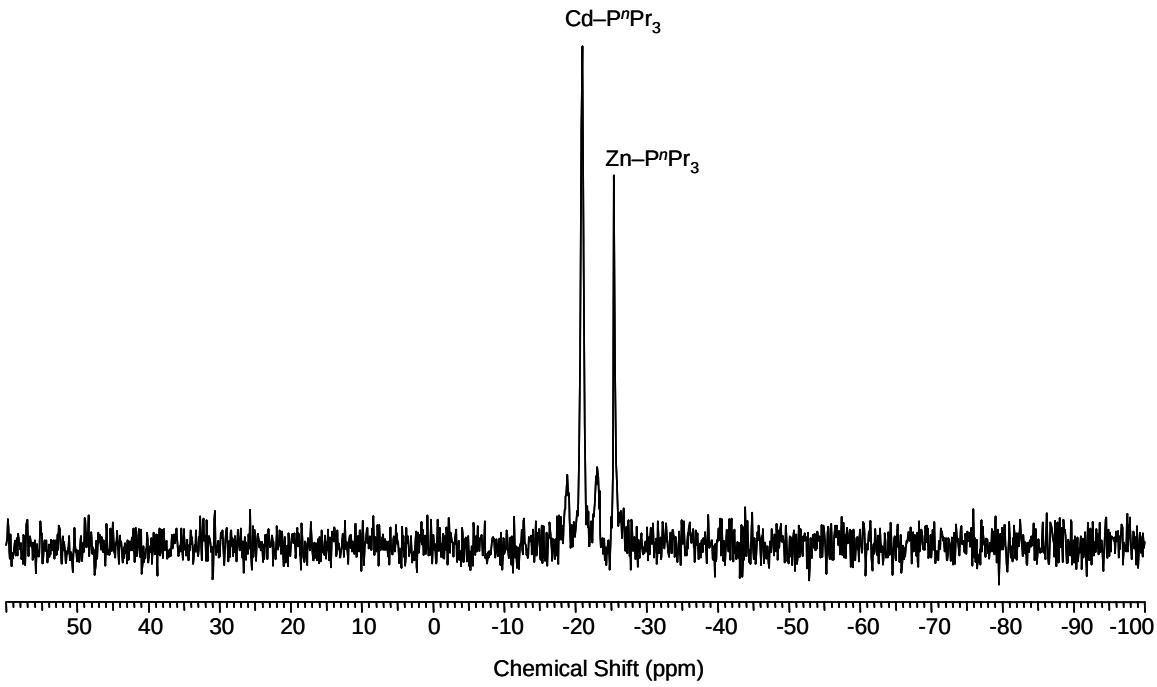

Figure S5. $^{31}P\{^1H\}$ NMR spectrum for complex **3b** in CD_2Cl_2 at room temperature.

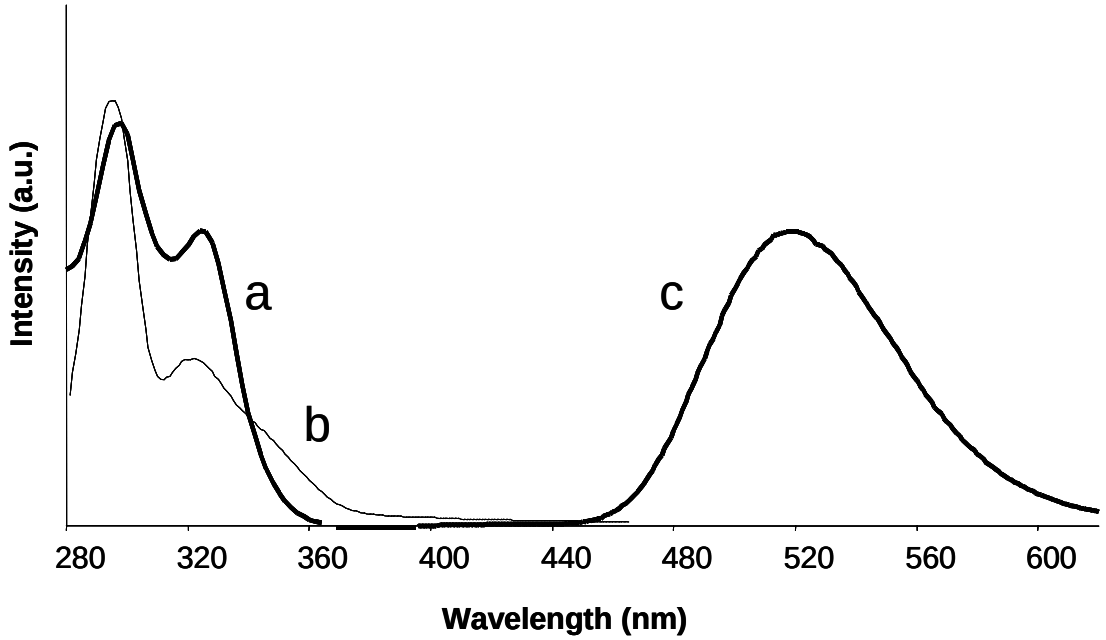

Figure S6. Absorption (a), photoluminescence excitation (b) and photoluminescence (c) spectra of cluster **3b** obtained as a frozen glass in 2-Me-THF at 77K.

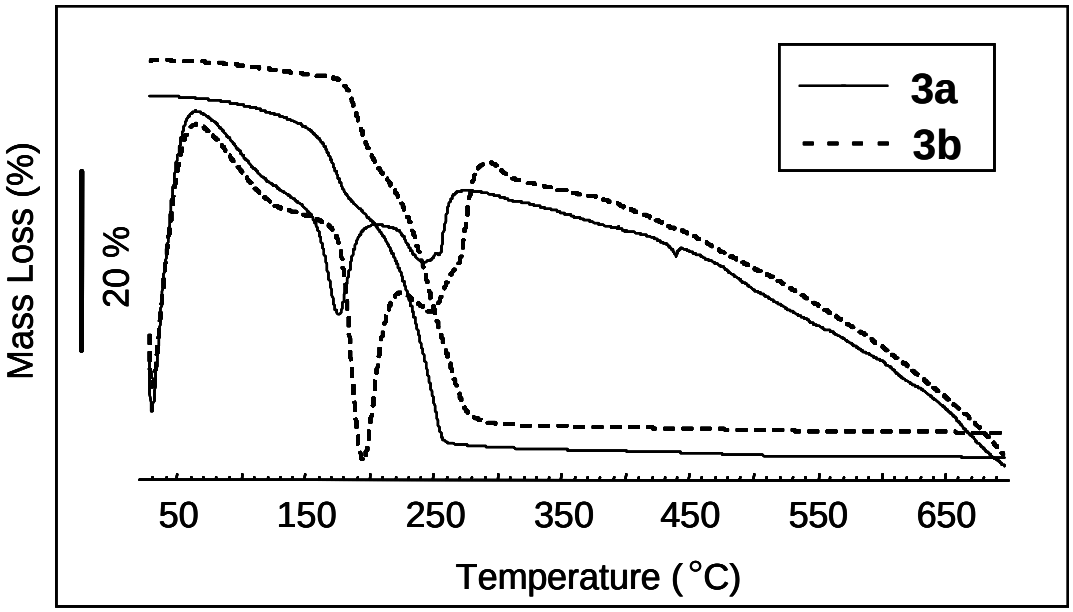

Figure S7. TGA and SDTA curves for the solid-state thermolysis of clusters **3a** (——) and **3b** (- - - - -).

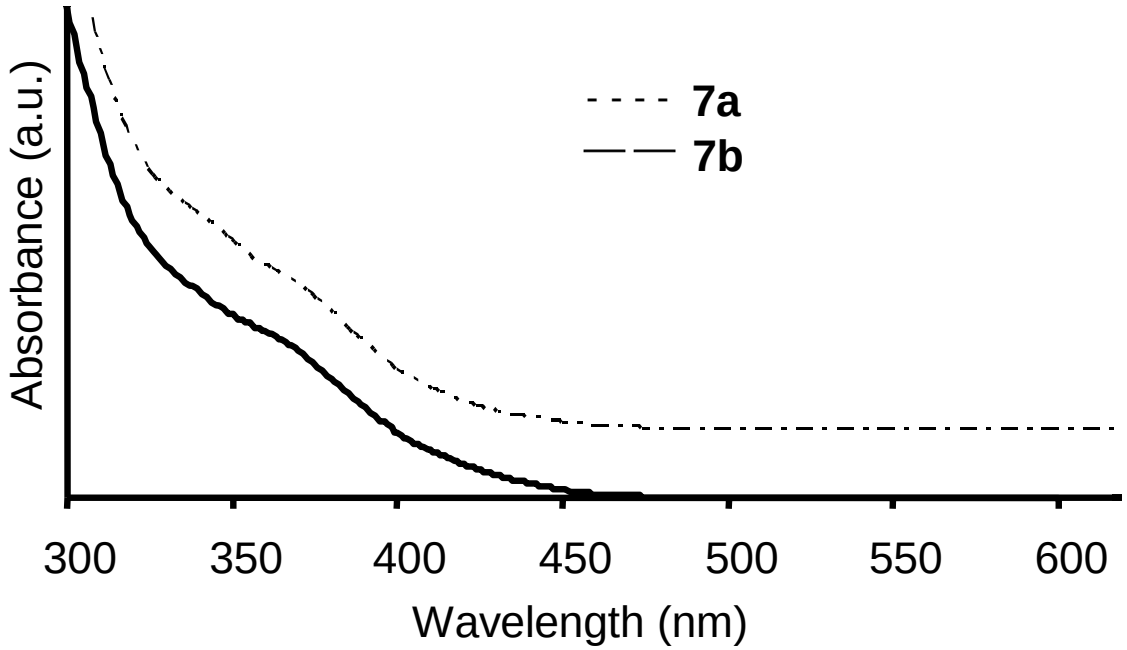

Figure S8. Room temperature solution (THF) absorption spectra of compounds **7a** and **7b**.

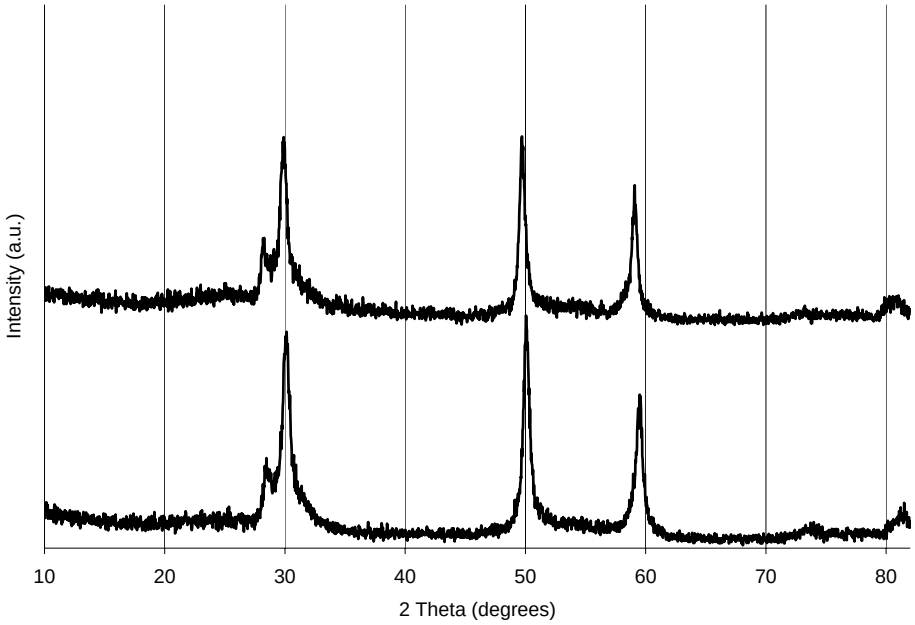

Figure S9. PXRD patterns for the residues remaining after thermolysis of clusters **2a** (top) and **2b** (bottom) to 700°C.

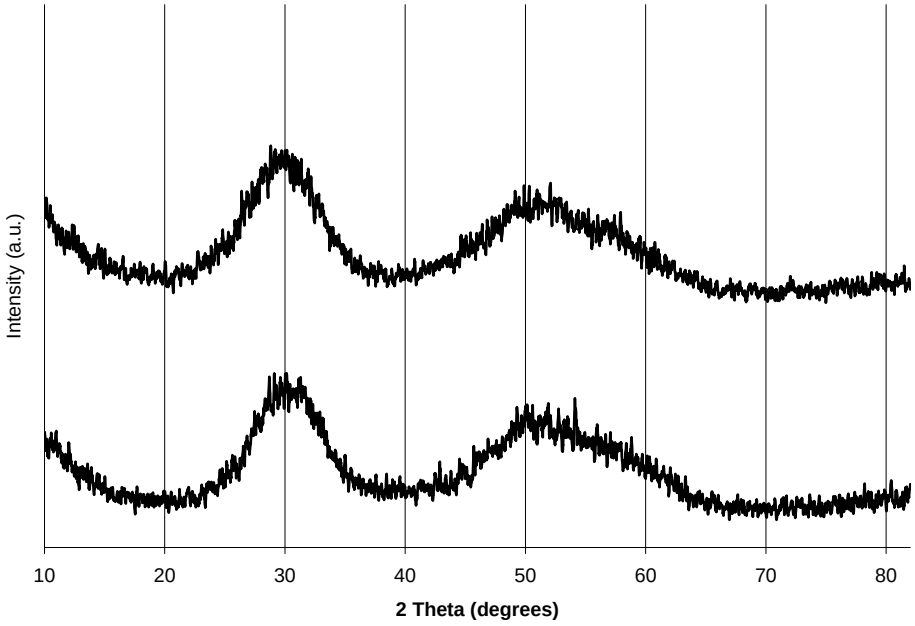

Figure S10. PXRD patterns for the residues remaining after thermolysis of clusters **2a** (top) and **2b** (bottom) to 250°C.

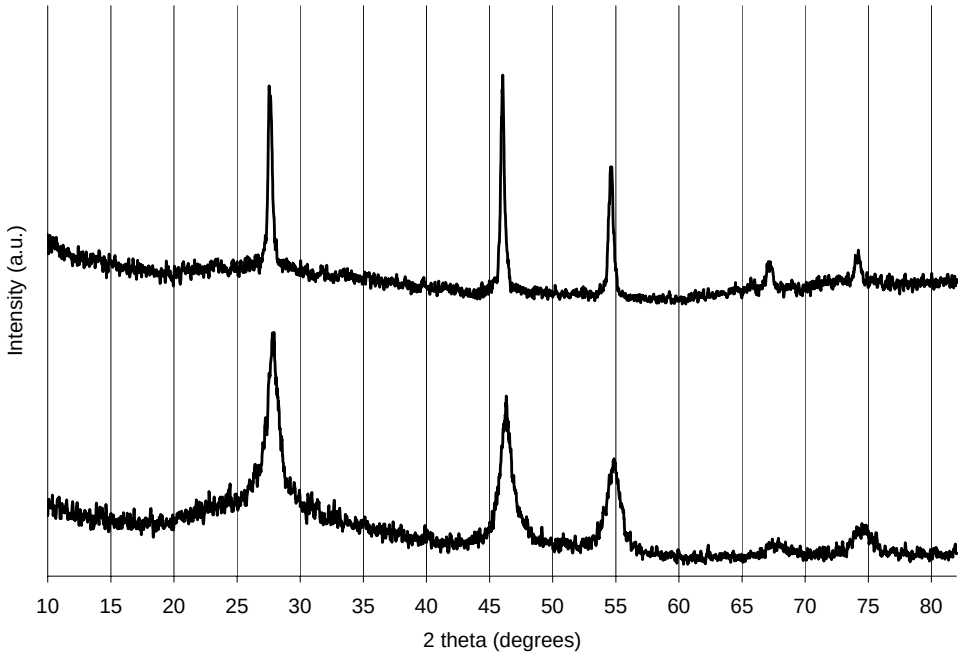

Figure S11. PXRD patterns for the residues remaining after thermolysis of clusters **3a** (top) and **3b** (bottom) to 250°C.

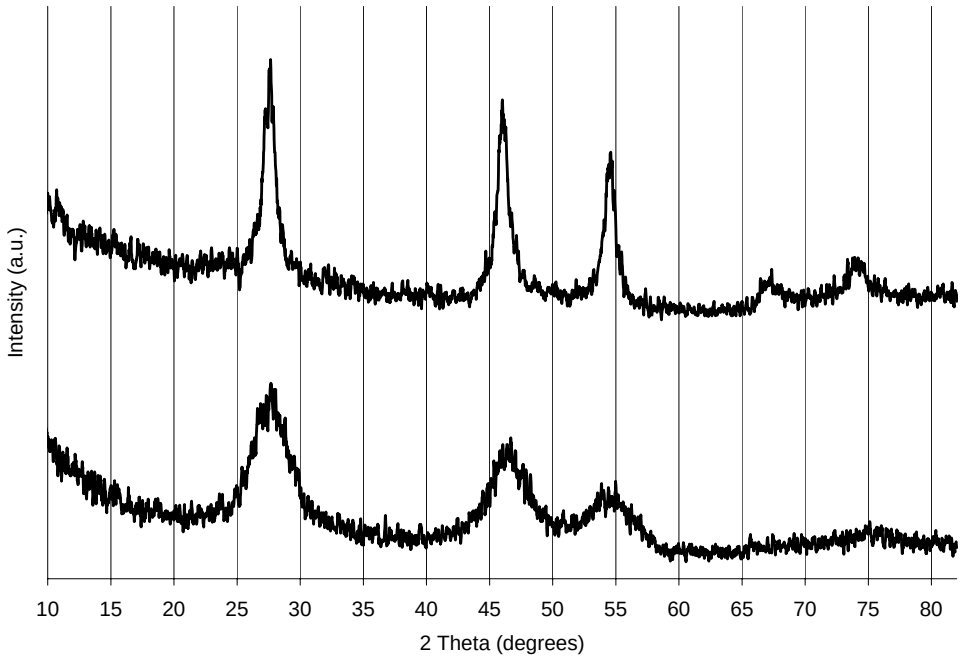

Figure S12. PXRD patterns for the residues remaining after thermolysis of clusters **3a** (top) and **3b** (bottom) to 200°C.

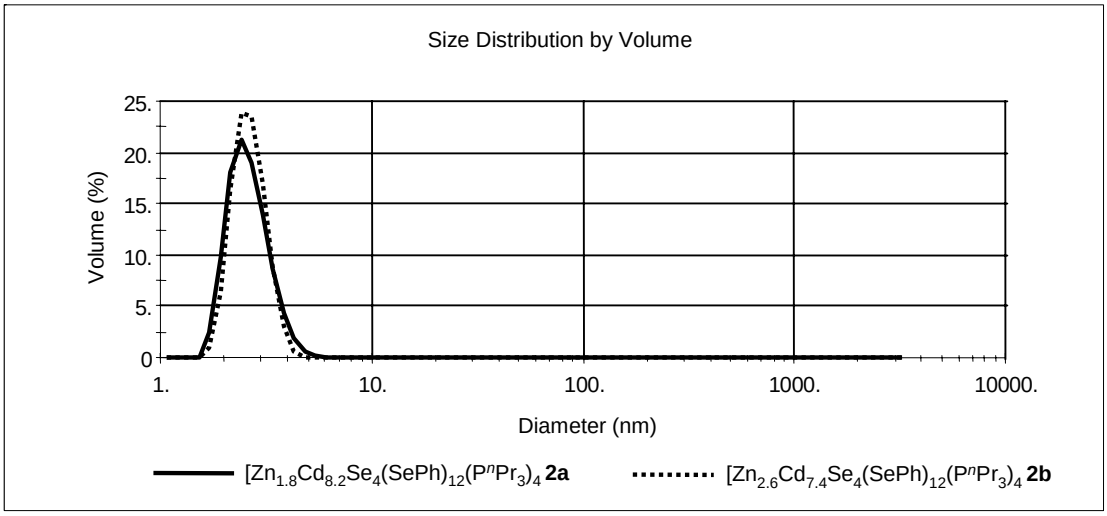

Figure S12. Dynamic light scattering particle size distributions for the residues remaining after thermolysis of clusters **2a** and **2b** to 250°C. Samples were dissolved in dichloromethane.